Source of surface ozone and reactive nitrogen speciation at Mount Waliguan in western China: New insights from the 2006 summer study

L. K. Xue,[1,2] T. Wang,[1,2] J. M. Zhang,[2] X. C. Zhang,[3] Deliger,[4] C. N. Poon,[2] A. J. Ding,[5] X. H. Zhou,[1] W. S. Wu,[2] J. Tang,[3] Q. Z. Zhang,[1] and W. X. Wang[1]

Received 9 July 2010; revised 6 December 2010; accepted 20 January 2011; published 14 April 2011.

[1] Surface ozone (O_3), carbon monoxide (CO), and total and speciated reactive nitrogen compounds (NO_y, NO, NO_2, PAN, HNO_3, and particulate NO_3^-) were measured at Mount Waliguan (WLG; 36.28°N, 100.90°E, 3816 m above sea level (asl)) in the summer of 2006 to further understand the sources of ozone and reactive nitrogen and to investigate the partitioning of reactive nitrogen over the remote Qinghai-Tibetan Plateau. The mean mixing ratios of O_3, CO, NO_y, and daytime NO were 59 ppbv, 149 ppbv, 1.44 ppbv, and 71 pptv, respectively, which (except for NO_y) were higher than those measured from a previous campaign in summer 2003, which is consistent with more frequent transport of anthropogenic pollution from central and eastern China in the measurement period of 2006 (55%) than that of 2003 (25%). The abnormally high values of NO_y observed in 2003 were suspected to be due to the positive interference from ammonia (NH_3) to the particular catalytic converter used in that study. Varied diurnal patterns were observed for the various NO_y components. The ozone production efficiencies ($\Delta O_3/\Delta NO_z$), which were estimated from the slope of the O_3-NO_z scatterplot, were 7.7–11.3 for the polluted plumes from central and eastern China. The speciation of reactive nitrogen was investigated for the first time in the remote free troposphere in western China. PAN and particulate NO_3^- were the most abundant reactive nitrogen species at WLG, with average proportions of 32% and 31%, followed by NO_x (24%) and HNO_3 (20%). The relatively large contribution of particulate NO_3^- to NO_y was due to the presence of high concentrations of NH_3 and crustal particles, which favor the formation of particulate nitrate. An analysis of backward trajectories for the recent 10 years revealed that air masses from central and eastern China dominated the airflow at WLG in summer, suggesting strong impact of anthropogenic forcing on the surface ozone and other trace constituents on the Plateau.

Citation: Xue, L. K., et al. (2011), Source of surface ozone and reactive nitrogen speciation at Mount Waliguan in western China: New insights from the 2006 summer study, *J. Geophys. Res.*, *116*, D07306, doi:10.1029/2010JD014735.

1. Introduction

[2] Ozone is an important trace gas in the troposphere for its roles in determining the oxidative capacity of the atmosphere, affecting human and vegetation health, and influencing the radiation budget of the atmosphere [e.g., *National Research Council*, 1991; *Intergovernmental Panel on Climate Change*, 2007]. The budget of ozone in the troposphere is determined by the downward transport of stratospheric air [*Stohl et al.*, 2003], dry deposition on the earth's surface, and photochemistry in the troposphere involving volatile organic compounds (VOCs) and nitrogen oxides (NO_x) [*Crutzen*, 1973].

[3] Reactive oxidized nitrogen compounds play a central role in the chemistry of the troposphere. They are emitted primarily as NO, followed by oxidation to NO_2 and other forms of oxidized nitrogen. Total reactive nitrogen (NO_y) is defined as the sum of NO_x (NO_x = NO + NO_2) and its atmospheric oxidation products and reactive intermediates (collectively abbreviated NO_z). NO_x, peroxyacetyl nitrate (PAN), nitric acid (HNO_3), and aerosol nitrate (NO_3^-) are the most abundant NO_y species, although their relative abundance can vary significantly [*Zellweger et al.*, 2003,

[1]Environment Research Institute, Shandong University, Ji'nan, China.
[2]Department of Civil and Structural Engineering, Hong Kong Polytechnic University, Hong Kong, China.
[3]Centre for Atmosphere Watch and Services, Key Laboratory for Atmospheric Chemistry, Chinese Academy of Meteorological Sciences, Beijing, China.
[4]China GAW Baseline Observatory, Qinghai Meteorological Bureau, Xining, China.
[5]Institute for Climate and Global Change Research, Nanjing University, Nanjing, China.

0148-0227/11/2010JD014735

references therein]. NO_x is usually dominant near its sources, whereas PAN tends to be more abundant in regionally polluted air masses that have undergone more active organic photochemistry. HNO_3 is the dominant component of NO_y in more remote areas of the troposphere [e.g., *Atlas and Ridley*, 1996; *Val Martin et al.*, 2008]. Besides, owing to its temperature dependent thermal decomposition and insoluble nature, PAN is usually more dominant than HNO_3 at colder and/or humid environments (i.e., at high altitudes and latitudes).

[4] In the Northern Hemisphere, emissions of reactive nitrogen are dominated by the anthropogenic sources in urban and industrial regions. After emitted, nitrogen oxides are photochemically processed and can be exported out of the planetary boundary layer, thereby affecting the ozone budget in distant downwind regions [*Wang et al.*, 1998]. The export of NO_x away from source regions is facilitated by the export of PAN, which can be transported long distances at cold temperatures and decomposed to NO_x in warmer environments [*Singh and Salas*, 1983; *Singh et al.*, 1986]. Similarly, the export of HNO_3 followed by its photolysis to NO_x, may also be an important source of NO_x even in the lower troposphere [*Neuman et al.*, 2006]. Thus, the measurement of NO_y and its constituents in the remote troposphere provides important information for understanding the impact of anthropogenic forcing on the global ozone budget.

[5] The Qinghai-Tibetan Plateau is the highest landmass on Earth, with an average altitude of over 4,000 m asl. The atmosphere lying over the Plateau is probably the least affected by human activities in the Asian continent due to the sparse population and minimal industrial activity in western China. A number of studies have been conducted at WLG on the northeastern edge of the Plateau on reactive trace gases, aerosols, and greenhouse gases [e.g., *Tang et al.*, 1995; *Ma et al.*, 2003; *Zhou et al.*, 2004; *Wang et al.*, 2006; *Mu et al.*, 2007; *Kivekäs et al.*, 2009]. A broad summer maximum of surface ozone has been observed at WLG [*Tang et al.*, 1995], which is in contrast to the common spring maximum pattern in most remote areas of the Northern Hemisphere [*Monks*, 2000]. Although field observations provided strong evidence of frequent intrusions of stratospheric air in summer [*Tang et al.*, 1995; *Ma et al.*, 2005; *Wang et al.*, 2006], chemical transport modeling studies suggested that anthropogenic effects from central and eastern China made a greater contribution to the summer ozone maximum at WLG [*Zhu et al.*, 2004; *Li et al.*, 2009]. In our 2003 study [*Wang et al.*, 2006], ozone rich air was found to be associated with low levels of water vapor and low concentrations of CO, which is a tracer of anthropogenic emissions, and meteorological simulations suggested an upper tropospheric/lower stratospheric source [*Ding and Wang*, 2006]. The 2003 study also observed abnormally high concentrations of NO_y at WLG compared with other remote environments, which was attributed to enhanced microbial processes in the soil over the Plateau [*Wang et al.*, 2006].

[6] To better understand the sources of summertime surface ozone and reactive nitrogen at WLG, another intensive campaign was conducted in the summer of 2006. Concurrent measurements of O_3, CO, NO_y, and its individual constituents (NO, NO_2, PAN, HNO_3, and NO_3^-) were taken. Compared with the previous summer campaign in 2003, the transport of anthropogenic pollution from central and eastern China was frequently observed during the study. Here, we present the results of this study. We first compare the data from 2006 with those from 2003 and examine the ozone production efficiencies in polluted air masses. We then examine the partitioning of NO_y and compare our results with those from other similar remote locations in the world. It is worth pointing out that this is the first time that NO_y partitioning data from the remote free troposphere in western China has been reported. We also conducted an analysis of the recent 10 years' back trajectories in order to derive the climatology of air mass transport in summer at WLG and to compare the 2006 and 2003 results with this long term mean.

2. Experiment and Methodologies

2.1. Site Description

[7] The field campaign was carried out at the WLG Observatory (36.28°N, 100.90°E, 3816 m asl) from 22 July to 16 August 2006. The station is one of 24 baseline observatories of the World Meteorological Organization's (WMO) Global Atmospheric Watch (GAW) program, which was developed to monitor long term trends in gaseous and aerosol parameters in the global free troposphere. The Observatory is situated on an isolated mountain peak at the northeastern edge of the Qinghai-Tibetan Plateau, and is far away from the main industrial and populated regions of China (see Figure 1). The closest cities with more than 10^6 inhabitants are Xining and Lanzhou, which are located 90 km to the northeast and 260 km to the east, respectively. More specific details on the site have been described elsewhere [e.g., *Ma et al.*, 2003; *Wang et al.*, 2006].

2.2. Measurement Techniques

[8] The measurement instruments were housed in a temperature controlled laboratory on the second floor of the station. The sampling system, instrumentation, and calibration procedures were similar to those used in 2003 [*Wang et al.*, 2006; *J. Zhang et al.*, 2009]. Only a brief summary is presented here, with an emphasis on several newly added instruments for the measurement of nitrogen containing species.

[9] O_3, CO, NO, NO_2, and PAN were sampled at 4.1 m above the rooftop of the building through a PFA tube (inside diameter: 9.6 mm; length: 10.2 m; total flow rate = 9.0 L/min), which was connected to a PFA made manifold in the laboratory. NO_y, HNO_3, and NO_3^- were sampled via two inlet boxes that housed catalytic converters and were placed at the sample intake point (2.1 m above the rooftop). The sample line connecting the catalytic box and the instrument has a length of 8.4 m and an inside diameter of 3.2 mm, with a flow rate of 1.5 L/min.

[10] O_3 was detected using a UV photometric analyzer (Thermal Environmental Instruments (TEI) Model 49C) with a time resolution of 1 min, a detection limit of 2 ppbv and a precision of 2 ppbv. CO was measured with a gas filter correlation nondispersive infrared analyzer (Advanced Pollution Instrumentation (API) Model 300) with a detection limit of 30 ppbv for a 2 min average and a precision of ~1% for a level of 500 ppbv. During the study, the baseline was determined every 2 h by passing ambient air to the internal CO scrubber for 15 min [*Wang et al.*, 2006].

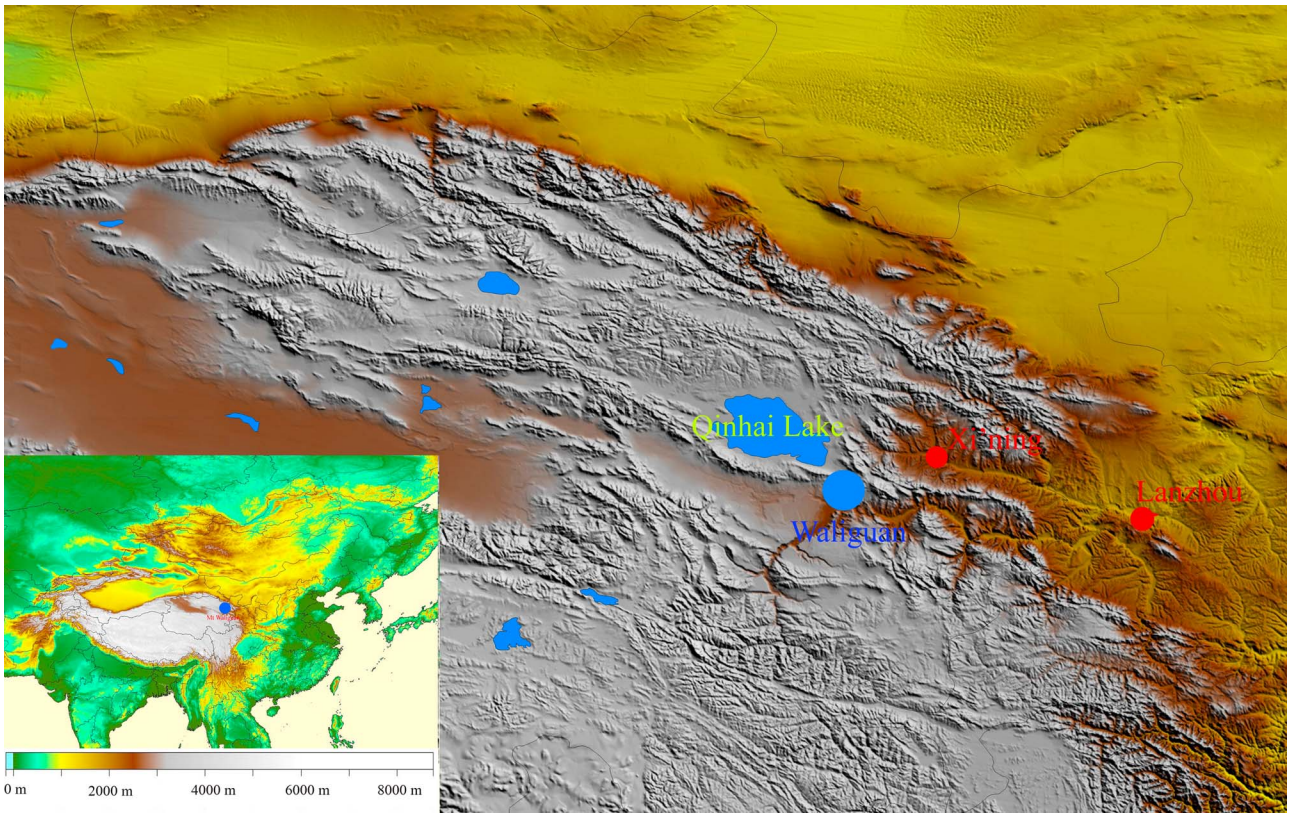

Figure 1. Topographical map (35°N–40°N, 95°E–105°E) showing the study site and surrounding regions.

[11] NO and NO_2 were measured using a chemiluminescence analyzer (Eco Physics, Model CLD 770 AL ppt) coupled with a photolytic converter (Eco Physics, Model PLC 760) by which NO_2 was converted to NO using a 300W, high-pressure, Xenon Arc lamp [*Wang et al.*, 2001]. The analyzer had a detection limit of 15 pptv for an integration time of 5 min, with a 2 σ precision of 10% and an uncertainty of 15%. The conversion efficiency of the photolytic converter was determined every 3 days by an NO_2 standard generated by the gas phase titration of NO with O_3, and ranged from 35% to 40% over the study period.

[12] NO_y was detected by another chemiluminescence analyzer (TEI, Model 42S) equipped with an externally placed molybdenum oxide (MoO) catalytic converter. NO_y was converted to NO on the surface of MoO at 350°C, and was then measured by the chemiluminescence detector [*Wang et al.*, 2006]. The detection limit of the analyzer was estimated to be 50 pptv for the time resolution of 1 min, with a 2 σ precision of 4% and an uncertainty of about 10%. The conversion efficiency of the MoO catalyst for NO_y species was checked daily by an n-propyl nitrate (NPN) standard that indicated the near complete (~100%) conversion of NPN throughout the campaign.

[13] HNO_3 and NO_3^- were measured by a third chemiluminescence analyzer (TEI, Model 42CY) in combination with two MoO converters. The measurement procedures were similar to that for NO_y, except that before entering the MoO converter, ambient air passed through a Teflon filter (which measures NO_y-NO_3^-) and another nylon filter to measure NO_y-HNO_3-NO_3^-. Laboratory and field studies have shown that gaseous HNO_3 can pass the upstream Teflon filter and would be efficiently collected by the downstream nylon filter [*Goldan et al.*, 1983; *Anlauf et al.*, 1986]. However, the efficiency with which HNO_3 penetrates the Teflon filter is highly dependent on the ambient RH and the particle loading on the filter. At WLG, the RH was generally low with daytime/nighttime mean values of 59% (±17%)/71% (±16%) during this study. Archived photos of weather conditions on the site reveal that there were few cloudy/foggy days during the campaign, with only several rainy events during which all the instruments were turned off. The Teflon and nylon filters were routinely changed in the morning every two days. Given the mean $PM_{2.5}$ concentration of 9.2μg/m^3 measured in the summer of 2003 [*Wang et al.*, 2006], assuming an increase of ~20% in 2006 (the same as CO) and a $PM_{2.5}$/TSP ratio of 0.6 [*Li et al.*, 2000], the particulate loading on the Teflon filter after two days was estimated as ~160 μg. Such particle loadings usually result in little retention (~10%) of HNO_3 [*Appel et al.*, 1981].The HNO_3 transmission efficiency is also expected to decrease with time after the filter replacement. Overall, we estimate the measurement uncertainties to be 20% for HNO_3 and 15% for NO_3^-. The detection limit of the detector was 50 pptv for 1 min data and 15 pptv for hourly averages.

[14] PAN was measured with a commercially available automatic PAN analyzer equipped with a calibration unit (Meteorologie Consult GmbH). The analytical method was based on gas chromatographic separation with sub-

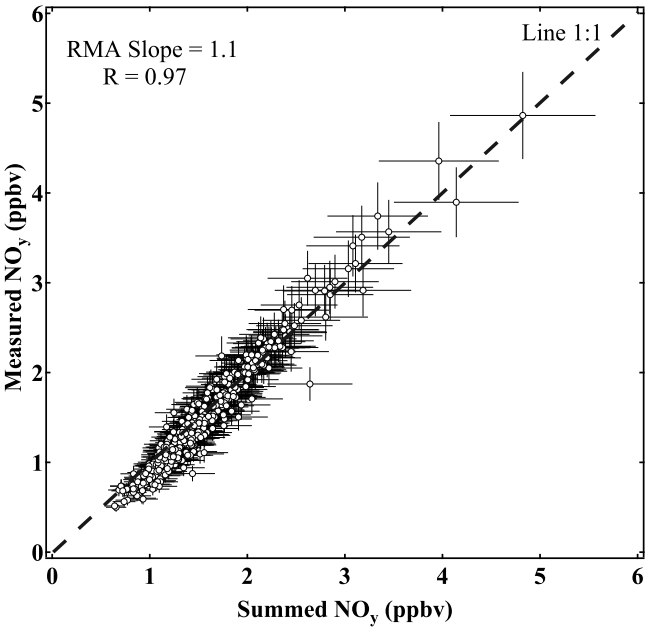

Figure 2. Comparison of the measured NO_y and the sum of individually measured constituents (NO_x, PAN, HNO_3, and NO_3^-). The error bars stand for the uncertainties within the specific measurements.

sequent electron capture detection (ECD). PC software (Adam32 v1.42) was used to control the sampling protocol and to collect the 10 min data. The analyzer had a detection limit of 50 pptv, with a 2 σ precision of 6% and an uncertainty of 15%. The instrument was calibrated weekly using the calibration unit. *J. Zhang et al.* [2009] provide further details of this instrument.

[15] The comparison of measured NO_y and the sum of its individual constituents can be used to check the accuracy of NO_y measurements. Generally, the summed NO_y is comparable to or reasonably smaller than the NO_y concentration [e.g., *Williams et al.*, 1997; *Zellweger et al.*, 2000]. In this study, the measured and summed NO_y values showed a good agreement (see Figure 2, r = 0.97), with an average $[NO_y]_{sum}/[NO_y]_{meas}$ ratio of 1.07. NO_x, PAN, HNO_3, and NO_3^- are believed to be the main reactive nitrogen compounds at WLG, accounting for ~100% of the total NO_y. The slightly higher value of the sum than the measured NO_y is due to the uncertainties of the different instruments used for the measurements.

[16] A data logger (Environmental Systems Corporation, Model 8816) was used to control the calibrations and to collect data (except for PAN), which were averaged over 1 min intervals. The data presented in this paper are hourly averaged values (except that 10 min data was used for the ozone production efficiency calculation). Various meteorological parameters are routinely monitored at the WLG Observatory [*Wang et al.*, 2006].

2.3. Calculation and Categorization of Backward Trajectories

[17] In the analysis of data collected in 2003, backward trajectories were calculated and further classified into several different groups to investigate the origins and transport pathways of air masses sampled at WLG [*Wang et al.*, 2006]. For the comparison with the 2003 study, we performed the same analysis for the 2006 study. Three-dimensional 10 day backward trajectories, terminated at 500 m above the ground level (AGL) of the peak of WLG, were calculated hourly using the Hybrid Single Particle Lagrangian Integrated Trajectory (HYSPLIT Model, version 4.8, 2010, from R. R. Draxler and G. D. Rolph, http://ready.arl.noaa.gov/HYSPLIT.php) with the GDAS meteorological data. We then applied cluster analysis to segregate the calculated trajectories into a number of groups using the hierarchical Ward's method with a squared Euclidean measure. The positions of the endpoints (i.e., longitude, latitude, pressure) at 3 h intervals along the 240 h trajectories were selected as the clustering variables. The cluster analysis was performed on a PC using the statistical software SPSS.

3. Results and Discussion

3.1. Data Overview

3.1.1. Air Mass Transport Regimes

[18] Time series of the trace gases and meteorological parameters for the study period is shown in Figure 3, together with the air mass categories deduced from cluster analysis of the backward trajectories. As expected, two main types of air masses were sampled during the study period. One was the air mass containing high levels of O_3 but low concentrations of CO and water (see Figure 3, e.g., 23–26 July), which is characteristic of air from the upper troposphere/lower stratosphere. The other was the air mass influenced by anthropogenic pollution, which was characterized by sharp rises in the levels of combustion tracer(s), specifically CO and/or NO_y (see Figure 3, e.g., 29 July and 4 and 7–11 August). Air masses of this type also contained relatively high amount of water but had generally lower O_3 mixing ratios.

[19] To further identify the origins and transport pattern of the sampled air masses, three dimensional 10 day backward trajectories were calculated and then classified into five groups using the cluster method. Figure 4 shows the mean trajectories of the five clusters plotted on the Asian anthropogenic CO emissions [*Q. Zhang et al.*, 2009]. Open circles on the trajectories represent 6 h intervals, with the marker size indicating the percentage of each cluster. The five air mass groups are described as follows. CA denotes air masses coming from the northwest, originating in Central Asia, passing over Kazakhstan and China's Xinjiang region and subsiding from the higher altitudes to the measurement site. SM denotes air masses coming from the north originating in western Siberia and Mongolia and passing in the lower troposphere over the Inner Mongolia and Gansu provinces of China. CSC denotes air masses coming from the southeast passing through the planetary boundary layer at lower speeds over southern and central China. CEC denotes air masses passing over eastern and central China at fast speeds in the lower troposphere. CWC denotes air masses originating in Xinjiang and passing over the Gansu and Qinghai provinces of China. It can be seen from the anthropogenic CO emissions that the trajectories coming from the west pass over a large remote area with very few anthropogenic emissions.

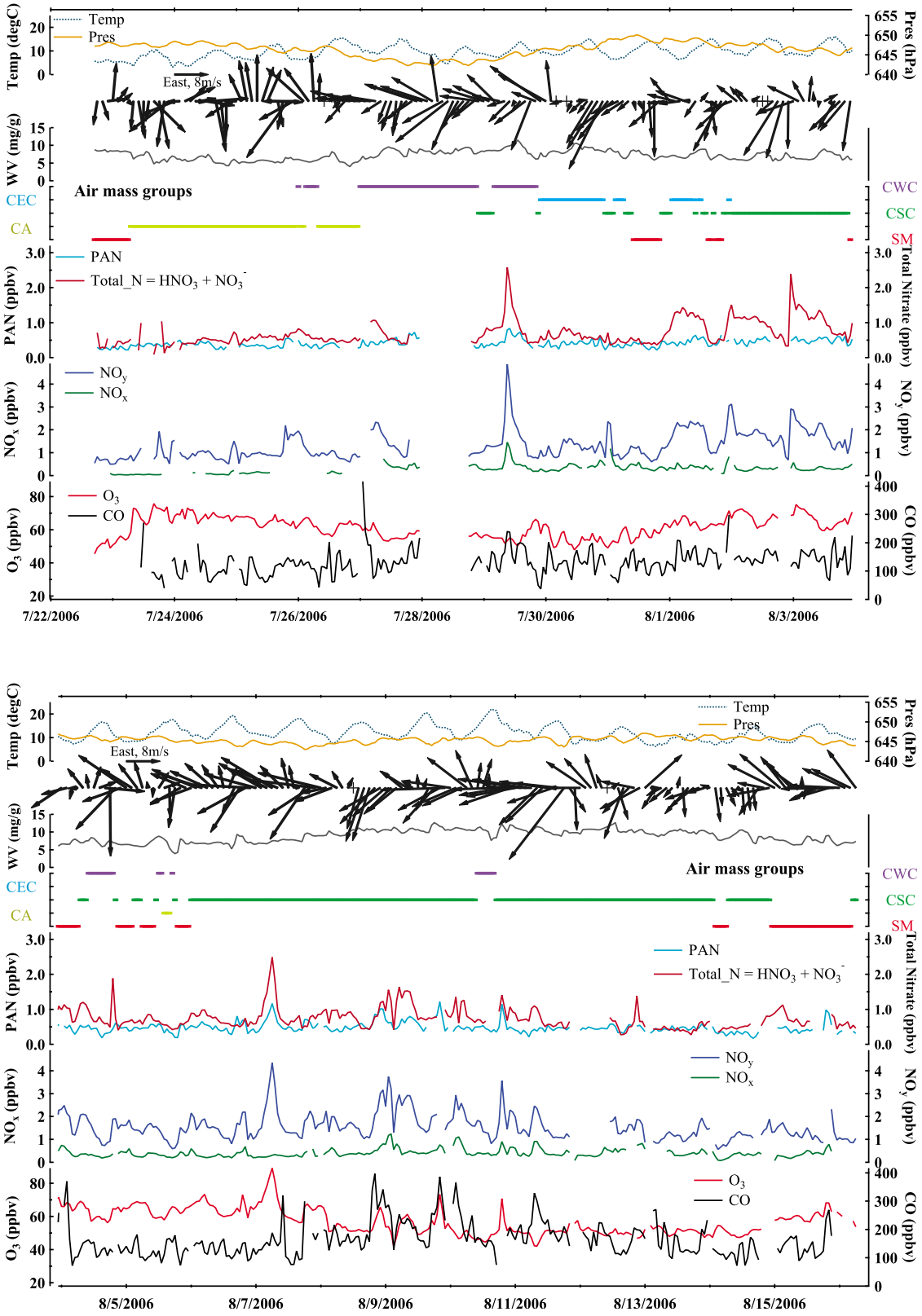

Figure 3. Time series of hourly data of trace gases and meteorological parameters measured at WLG between 22 July and 16 August 2006. The air mass groups are deduced from cluster analysis of the 10 day backward trajectories: SM, Siberia/Mongolia; CA, central Asia; CSC, central/southern China; CEC, central/eastern China; and CWC, central/western China.

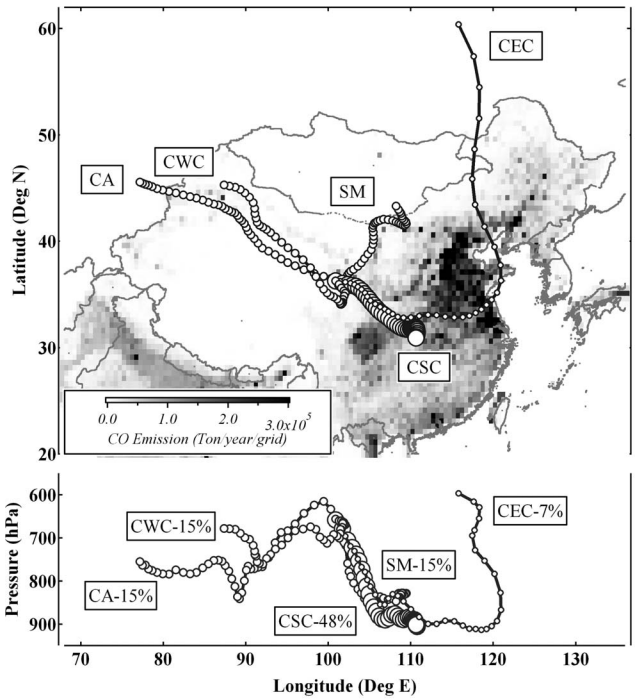

Figure 4. Mean 10 day backward trajectory clusters plotted on the Asian anthropogenic CO emissions (http://www.cgrer.uiowa.edu/EMISSION_DATA_new/data/intex b_emissions/). The open circles on the trajectories indicate 6 h intervals. The size of the markers indicates the percentage of each cluster.

[20] Among the five groups identified, CSC occurred the most, accounting for 48% of the total, followed by CA (15%), SM (15%), CWC (15%), and CEC (7%). The majority of air masses (e.g., CSC and CEC, 55%) had passed over the populated regions of China before arriving at the site, suggesting extensive transport of anthropogenic pollution to the Plateau during the study period. This is quite different from the transport pattern encountered in the summer study of 2003, in which most air masses came from the west (e.g., CA 37% and EU Trop 13%) and only a small fraction passed over central and southern China (e.g., SC 25%) [*Wang et al.*, 2006]. These results indicate significant year to year variability in the large scale dynamics.

[21] To learn about the typical air mass transport pattern at WLG in summer, we calculated 10 day backward trajectories every 3 h for the summer months (15 July to 17 Aug) in the recent 10 years (2000–2009). The cluster approach was then applied to the whole of trajectories to picture the climatological transport pathways of air masses. Three types of transport pathways were identified, representing three major directions from which air parcels came to the site. Table 1 gives percentages of three air mass types for the period of 2000–2009 and for the 2 years during which the field campaigns took place. Over the recent 10 years, the transport regime at WLG in summer was dominated by the air coming from the east (~49%) that may have passed over the populated regions of China, with 26% of air masses from the remote west and 25% from the north. Comparing against this 'long term' averaged pattern, the summer 2006 had more frequent transport from the east (63%) and less from the west (20%) whereas 2003 had less impact from the east (37%) but much more from the west (44%). The reduced transport from the east in 2003 may have been due to a weaker summer monsoon in 2003 [e.g., *Ogi et al.*, 2005; *Saigusa et al.*, 2010].

3.1.2. Concentrations in 2006

[22] Table 2 summarizes the statistics of trace gases for the whole data set and for subdivisions of the upslope (0800–1959 local time (LT)) and downslope (2000–0759 LT) observations according to changes in vertical winds (see Figure 5). The mean levels of trace gases (except for NO_y) were higher than those measured in the previous campaign in summer 2003. In the 2006 study, the average concentrations of O_3, CO, and NO (daytime data) were 59 ppbv, 149 ppbv, and 71 pptv, respectively, compared with the respective mean values of 54 ppbv, 125 ppbv, and 47 pptv in 2003 [*Wang et al.*, 2006]. The *t* tests suggest the differences in the levels of trace gases between the two periods to be statistically significant ($p < 0.01$). However, the values of NO_y (mean = 1.44 ppbv) were much lower than those in 2003 (mean = 3.60 ppbv), which is further discussed in section 3.3.1. A discussion of the relative abundance of the individual NO_y components is given in section 3.3.2.

[23] We also examined the chemical characteristics of the five air mass groups by sorting the hourly data on trace gases and water vapor according to the trajectory clusters. The statistical results are given in Table 3. The air masses from the western remote regions (CA) contained the lowest levels of CO (mean = 110 ppbv) and NO_y (mean = 1.04 ppbv), the least amount of water (mean = 5.9 mg/g), but the highest O_3 mixing ratios (mean = 66 ppbv). Indeed, the CA air mass was in good correspondence with the measurements potentially influenced by the upper tropospheric/lower stratospheric air as examined in Figure 3 (e.g., 23–26 July). In contrast, the other air masses that were possibly influenced by anthropogenic pollution had high concentrations of CO (mean = 136–166 ppbv) and NO_y (mean = 1.18–1.65 ppbv), a relatively higher amount of water (mean = 7.3–8.8 mg/g), and lower O_3 mixing ratios (mean = 57–60 ppbv).

3.1.3. Diurnal Variations

[24] At WLG, weak diurnal variations were observed for O_3, CO, and reactive nitrogen oxides. Figure 5 shows the average diurnal patterns of trace gases and surface winds

Table 1. Percentage of Three Major Types of Air Masses at WLG in the Summer Months of 2000–2009[a]

Period	East[b]	West[b]	North[b]
2000–2009	49%	26%	25%
2003	37%	44%	19%
2006	63%	20%	17%

[a]Ten day backward trajectories terminating at 500 m (AGL) above the peak of WLG were calculated every 3 h by the HYSPLIT model for the period of 15 July to 17 August in the year of 2000–2009. The same cluster approach (see section 2.3) was used to segregate the trajectories into specific clusters.

[b]Three major air masses: "East" contains air masses coming from the east and southeast that have passed over the populated regions of China (i.e., CSC and CEC in Figure 4); "West" contains air masses coming from the west, passing over the remote regions of central Asia and Xinjiang (i.e., CA); and "North" contains air masses coming from the north and mainly passing over Siberia and Mongolia regions (i.e., SM).

Table 2. Statistics on Hourly Data of Trace Gases Measured at WLG[a]

Species	All Data		Upslope[b]		Downslope[b]	
	Mean	N	Mean	N	Mean	N
O_3	59 (8)	558	58 (7)	280	61 (8)	278
CO	149 (57)	506	142 (50)	267	156 (64)	239
NO_y	1.44 (0.61)	540	1.37 (0.56)	273	1.51 (0.66)	267
NO	40 (47)	421	71 (45)	223	4 (14)	198
NO_2	0.32 (0.18)	478	0.28 (0.13)	257	0.36 (0.22)	221
PAN	0.44 (0.14)	524	0.44 (0.13)	265	0.45 (0.15)	259
HNO_3	0.26 (0.09)	511	0.26 (0.11)	264	0.26 (0.08)	247
NO_3^-	0.48 (0.32)	525	0.43 (0.32)	260	0.53 (0.31)	265
NH_3*[c]	7.9 (4.0)	535	8.0 (3.8)	269	7.8 (4.2)	266

[a]The mean (standard deviation) values are in ppbv, except for NO, which is in pptv. N is the number of hourly data points.

[b]Upslope equals 0800–1959 local time (Beijing time); downslope equals 2000–0759 local time.

[c]NH_3* equals $NH_3 + NH_4^+$, which was measured by the NO_y detector with MoO conversion at 450°C.

(both horizontal and vertical) in the 2006 study. Similar to other mountaintop sites, local anabatic (represented by positive speeds) and catabatic winds are clearly shown at WLG. For trace gases, the mean O_3 mixing ratios showed a trough around noon (1000–1400 LT) with a minimum of ~56 ppbv, and enhanced levels at nighttime with a maximum of ~62 ppbv. The average concentrations of CO and NO_y were lower (CO = 120 ppbv; NO_y = 1.0 ppbv) in the afternoon and higher (CO = 150–175 ppbv; NO_y = 1.6–1.7 ppbv) in the morning and at night. The diurnal patterns of CO and O_3 were similar to those measured in the 2003 summer study [*Wang et al.*, 2006], but the NO_y profile was quite different from that in 2003, which showed a broad daytime maximum pattern with much higher values.

[25] Varied diurnal patterns were observed for individual NO_y species due to their different properties in transport, chemical transformation, and removal processes. NO_3^- had a similar profile to NO_y, with lower levels (~0.25 ppbv) in the afternoon and higher concentrations (0.6–0.7 ppbv) in the morning and at night. PAN also had an afternoon trough (~0.37 ppbv), and showed an apparent peak (~0.56 ppbv) in the evening (~2000 LT) which was mainly caused by several plumes transported from the urban areas of Lanzhou [*J. Zhang et al.*, 2009]. In contrast, the average HNO_3 concentrations showed a maximum (~0.32 ppbv) in the afternoon (1400–1600 LT), implying the in situ production of HNO_3 with higher levels of OH and/or evaporation of NO_3^- to HNO_3 at high temperatures (as evinced by the coinciding sharp decrease in NO_3^-). As for NO_2, the mixing ratios exhibited a maximum (~0.45 ppbv) at nighttime, with a relatively smaller peak (~0.35 ppbv) in the morning (0900 LT) and lower levels (~0.25 ppbv) in the early morning (0600 LT) and afternoon. The NO levels showed a broad daytime maximum pattern (~115 pptv) that was due to the photolysis of NO_2 to NO. These daytime concentrations also imply that the NO levels at WLG are sufficiently high to sustain a net ozone photochemical production [*Duderstadt et al.*, 1998].

3.2. Ozone Production Efficiency in Polluted Air Masses

[26] It is of interest to investigate how efficient O_3 is formed during the oxidation of NO_x in the air masses with recent influence of anthropogenic emissions from the east.

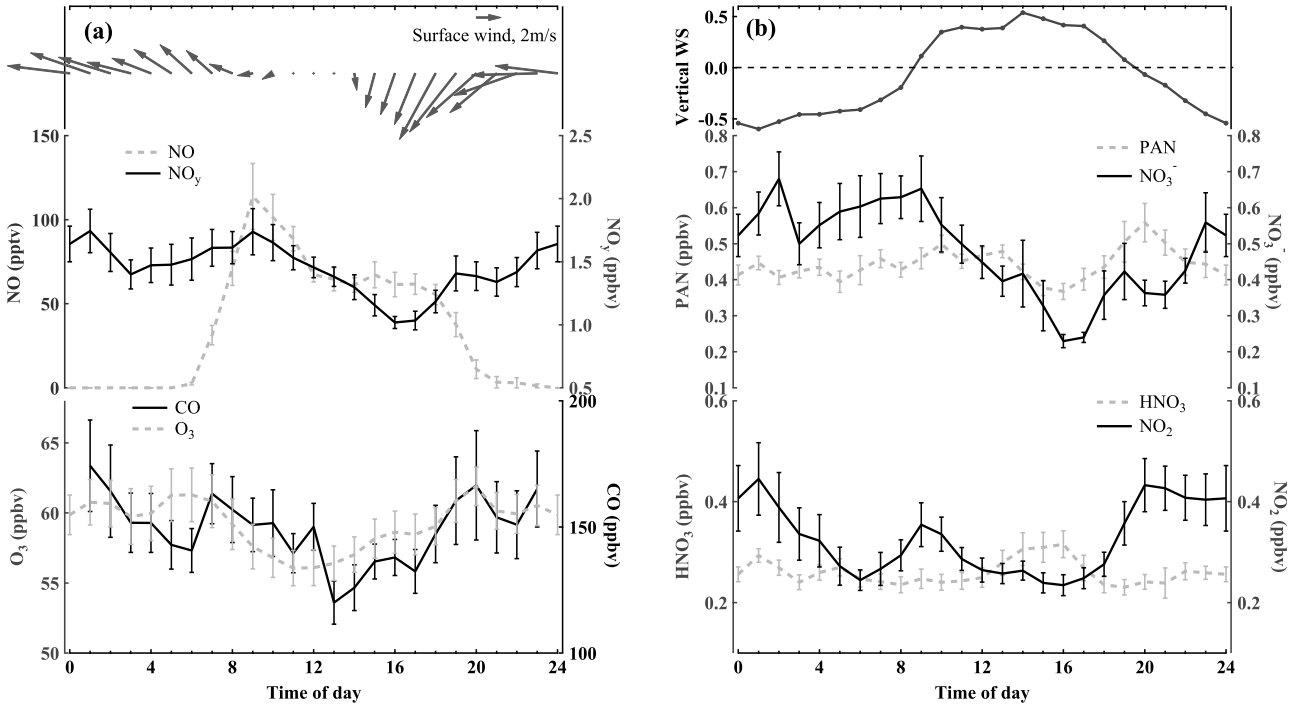

Figure 5. Average diurnal profiles of (a) NO, NO_y, and other trace gases and (b) reactive nitrogen compounds at WLG. Diurnal patterns of surface winds (both horizontal and vertical) are also given. The error bars indicate the standard errors of the measurement data.

Table 3. Classification of Trace Gases and Water Vapor in the Different Air Mass Groups[a]

Air Mass	O_3	CO	NO_y	NO_x	PAN	HNO_3	NO_3^-	NH_3*	WV
CA	66 (4)	110 (40)	1.04 (0.44)	0.10 (0.06)	0.36 (0.07)	0.20 (0.05)	0.40 (0.32)	4.4 (1.0)	5.9 (1.0)
SM	60 (6)	138 (51)	1.18 (0.45)	0.32 (0.17)	0.40 (0.14)	0.24 (0.08)	0.37 (0.19)	5.7 (1.7)	7.3 (0.9)
CSC	58 (8)	166 (60)	1.65 (0.59)	0.40 (0.19)	0.49 (0.15)	0.28 (0.10)	0.53 (0.32)	9.7 (4.5)	8.8 (1.8)
CEC	58 (6)	136 (48)	1.47 (0.57)	0.38 (0.14)	0.41 (0.09)	0.27 (0.06)	0.52 (0.29)	8.1 (2.2)	8.1 (1.2)
CWC	57 (5)	146 (50)	1.43 (0.72)	0.41 (0.22)	0.45 (0.13)	0.28 (0.12)	0.51 (0.40)	7.5 (2.8)	8.1 (1.5)

[a]Values are given as means (standard deviations) in ppbv, except for water vapor (WV), which is in mg/g.

Ozone production efficiency (OPE) is defined as the number of ozone molecules produced per molecule of NO_x oxidized, and is empirically inferred from the regression slope of the observed scatterplot of O_3 versus NO_z [*Trainer et al.*, 1993]. It's worth noting that the slope is also affected by the relative removal rates of O_3 and NO_z (especially the rapid deposition of HNO_3) and by the mixing of different air masses [*Zanis et al.*, 2007]. Thus, the slope of an O_3-NO_z scatterplot generally provides only the upper limit of the gross ozone production efficiency.

[27] To exclude the interference from mixing with highly processed free tropospheric air, we only selected several polluted plumes with recent anthropogenic influences using the measured atmospheric NO_y/CO ratios, which have been used to discriminate between disturbed and undisturbed free tropospheric conditions at Jungfraujoch [*Zellweger et al.*, 2003]. The NO_y/CO ratio generally decreases with the lifespan of an air parcel due to the longer life time of CO than NO_y. *Jaeglé et al.* [1998] reported an average NO_y/CO ratio of ~0.1 in air close to anthropogenic sources and of ~0.005 in the upper troposphere. In the present study, the polluted air masses were identified if the following criteria were fulfilled. (1) The air masses had passed over the populated central and eastern regions of China before arriving at the site (belonging to CSC and CEC air mass groups); (2) there was no shift in wind directions during the pollution events; (3) the NO_y/CO ratios were higher than 0.01; and (4) concurrent measurements of O_3, NO_y and NO_x were available. Five plumes with enhancements of ozone (and other pollutants) were finally extracted for the further analysis. They were observed during 3, 6, 7, 9, and 10 August (see Figures 3 and 6).

[28] Figure 6 shows the O_3-NO_z scatterplots for 10 min data for all the five polluted plumes. The slopes were in the range of 7.7–11.3 ppbv/ppbv, with a mean value of 9.9 (±1.7). Note that the slopes were determined with the reduced major axis (RMA) method to take into account measurement uncertainties in both the x and y variables [*Hirsch and Gilroy*, 1984]. These values are somewhat higher than those observed in urban and rural areas, and are comparable to the observations made at other remote continental sites. For example, *Wang et al.* [2010] observed OPE values of ~3 at both an urban and a downwind mountainous site of Beijing in summer 2008. *Chin et al.* [1994] reported an average OPE value of 5.5 in the U.S. boundary layer with values being more than 2 times higher in the west (9.1) compared to the east (4.2). *Wood et al.* [2009] derived an OPE value of 6.2 at a mountaintop site within the Mexico City Basin during a stagnant ozone episode with an extremely large ozone production rates. At Jungfraujoch, *Zanis et al.* [2007] calculated OPE values of 7–9 for polluted air masses in summer months, compared to the higher values of 15–20 for highly processed free tropospheric air.

3.3. Reactive Nitrogen Chemistry

3.3.1. Lower Concentrations of NO_y Than in 2003

[29] One objective of the present study was to reexamine the atmospheric levels and source(s) of reactive nitrogen at WLG. In the previous study in 2003, we found that the concentrations of NO_y at WLG were abnormally high (means = 3.60–3.83 ppbv) compared with those at other remote sites [*Wang et al.*, 2006]. Soil emissions enhanced by the presence of animal waste were proposed to be an important factor. During the 2006 study, the NO_y levels were much lower (mean = 1.44 ppbv) than those observed in 2003 despite the more frequent transport of polluted air masses. In this section, we discuss the possible reasons for the difference in NO_y levels between the two studies by examining both changes in emissions and measurement interference.

[30] Soil emissions of NO_x (as NO) are closely related to temperature, precipitation, and soil type [*Williams et al.*, 1988; *Yienger and Levy*, 1995]. The amount of NO released increases with the surface temperature, precipita-

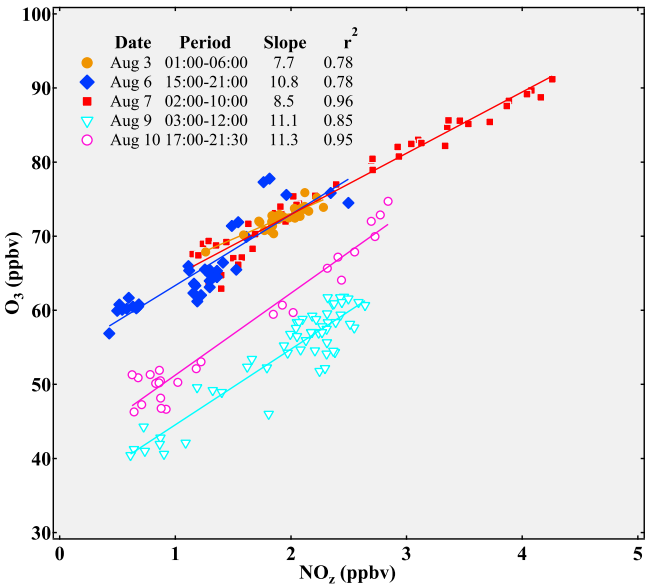

Figure 6. Scatterplots of ozone versus NO_z for the 10 min data for the identified five plumes with recent anthropogenic influences from central and eastern China. The regression lines were obtained with the reduced major axis method.

Table 4. Comparison of the NO_y Budget at WLG With Those Obtained From Other Remote, High-Altitude Sites in the Northern Hemisphere

Site	Location	Altitude (m asl)	Period	NO_y Partitioning				NO_y (pptv)	Reference[a]
				NO_x	PAN	HNO_3	NO_3^-		
WLG	36.28°N, 100.90°E	3816	22 Jul to 16 Aug 2006	0.24	0.32	0.20	0.31	1439	1
Jungfraujoch	46.55°N, 7.98°E	3580	18 Jul to 23 Aug 1997	0.22	0.36	0.07	0.17	986	2
Idaho Hill	39.5°N, 105.37°W	3070	24 Sep to 4 Oct 1993	0.66	0.19	0.09	0.06	1759	3
Mauna Loa	19.54°N, 155.58°W	3400	15 Jul to 15 Aug 1992	0.14	0.04	0.35	0.13	203	4
Pico Mountain	38.47°N, 28.40°W	2200	20 Jul 2002 to 25 Aug 2005 (summer)	0.12	0.21	0.71		365	5
Summit, Greenland	72.33°N, 38.75°W	3210	3–16 Jul 1999	0.33	0.55			50~350	6
Summit, Greenland	72.55°N, 38.4°W	3200	May-Jul 1995			0.01		850	7
Goose Bay, Labrador	53.3°N, 60.4°W	2000–4000	Jul-Aug 1990	0.15	0.77	0.29	0.04	330	8
Western Pacific Ocean	25°N–42°N	3000–7000	Sep-Oct 1991	0.18	0.20	0.25	0.13	376	9
TRACE P (costal)	20°N–40°N, 90°E–130° E	2000–7000	Feb-Apr 2001	0.06	0.24	0.69		475	10
INTEX A (North America)	25°N–55°N, 140°W–40°W	2000–4000	1 Jul to 15 Aug 2004	0.08	0.26	0.60	0.14	809	11

[a]References: 1, this study; 2, *Zellweger et al.* [2000]; 3, *Williams et al.* [1997]; 4, *Atlas and Ridley* [1996]; 5, *Val Martin et al.* [2008]; 6, *Ford et al.* [2002]; 7, *Munger et al.* [1999]; 8, *Singh et al.* [1994]; 9, *Singh et al.* [1996]; 10, *Talbot et al.* [2003]; and 11, *Singh et al.* [2007].

tion frequency, and nitrate and ammonium content of the soil. In the 2006 study, the average temperature (±standard deviation) at WLG was 10.9(±3.4)°C, which was even slightly higher than that of 9.3(±3.5)°C in the summer campaign of 2003. According to our on-site observations, there was no significant decrease in rainfall events between the study periods (five events in 2006 versus six events in 2003). On the Qinghai Tibetan Plateau, animal feces are a major source of the N substances in the soil. In 2006, there were about 23 million livestock in Qinghai province, which is also similar to the number in 2003 [*Qinghai Bureau of Statistics*, 2007]. It can thus be concluded that the difference in NO_y levels between the 2 years is unlikely to be due to changes in soil emissions.

[31] As to anthropogenic emissions, the NO_x emissions in China had increased by 55% from 2001 to 2006, with the greatest growth occurring in the eastern part of the country [*Zhang et al.*, 2007; *Q. Zhang et al.*, 2009]. Qinghai province had also undergone rapid economic development, with energy consumption and the number of motor vehicles increasing sharply by 70% and 43%, respectively, during the period 2003 to 2006 [*Qinghai Bureau of Statistics*, 2007]. The available emission data [*Streets et al.*, 2003; *Q. Zhang et al.*, 2009] also indicates an upward trend (~16%) in the NO_x emissions in "Qinghai" (domain: Latitude 33°N–39°N, Longitude 90°E–102°E) over the period 2000 to 2006. It can thus be expected that anthropogenic emissions should have increased between the study periods. Other sources such as biomass burning and lighting are not expected to sustain the high levels of NO_y in 2003 [*Wang et al.*, 2006].

[32] It is known that measurements of NO_y using catalytic converters can be subject to positive interference due to the conversion of non-NO_y nitrogen compounds such as NH_3. Previous studies have reported an average conversion efficiency of about 10% for NH_3 (range: 0–26%) based on testing a suite of MoO converters [*Williams et al.*, 1998; *Fitz et al.*, 2003]. The conversion efficiency of NH_3 has been found to be independent of temperature, but to rise as the converter ages (note that in both of our studies, all of the converters were newly installed at the beginning of the measurement period). To further determine the interference from NH_3 in the NO_y measurements, we tested four MoO converters of different ages in a recent field study by spiking them 49 ppbv of NH_3. Out of the four converters, three converted NH_3 at an efficiency of 0–14%, which is consistent with the previously reported results. However, a new converter showed an extremely high conversion efficiency of ~38% at 350°C but this decreased to ~11% at 325°C. This suggests that new converters may also be subject to strong interference by NH_3.

[33] At WLG, the concentrations of NH_3* (measured as $NH_3+NH_4^+$ by MoO conversion at 450°C) were relatively high, with an average value (±standard deviation) of 7.9 (±4.0) ppbv during the present study. A passive sampling study also showed a summertime NH_3 level of ~4 ppbv [*Meng et al.*, 2010]. If we assume a very high (30%) conversion efficiency in the catalytic converter used in the 2003 study and the same levels of NH_3* as in 2006, the positive interference could have been as large as 2.4 ppbv in 2003, which is sufficiently high to explain the discrepancy in NO_y levels between the two studies. We have no solid evidence to indicate that this actually occurred, there is, however, a possibility that the very high NO_y levels in 2003 were in large part due to NH_3 interference in the particular converter used in that study.

[34] Although the mean NO_y level in the 2006 study was much lower than those in the previous campaigns in 2003, it was still higher than the mean levels measured at other remote sites (see Table 4, and see also Table 2 of *Wang et al.* [2006]). For example, values of 1.15 ppbv were observed at Mount Cimone (Italy, 2165 m asl), 0.99 ppbv at Mount Jungfraujoch (Switzerland, 3580 m asl), 0.81 ppbv and 0.48 ppbv on INTEX A and TRACE P aircrafts. Much lower concentrations were measured at Mauna Loa (0.20 ppbv, Hawaii, 3400 m asl) and Pico Mountain (0.37 ppbv, Azores, 2200 m asl). However, it was lower than the mean concentrations measured at Idaho Hill (1.76 ppbv, U.S., 3070 m asl) and Niwot Ridge (2.0 ppbv, U.S., 3050 m asl), both of which are relatively close to urban sources.

Table 5. Average Proportions of Individual NO_y Species at WLG[a]

Data Set	N	NO_x/NO_y	PAN/NO_y	NO_3^-/NO_y	HNO_3/NO_y
All data	404	24% (10%)	32% (8%)	31% (9%)	20% (9%)
Upslope[b]	221	25% (9%)	34% (8%)	29% (9%)	20% (10%)
Downslope[b]	183	23% (11%)	30% (8%)	34% (8%)	19% (7%)
CA	33	12% (6%)	38% (7%)	38% (10%)	23% (7%)
SM	61	24% (10%)	34% (9%)	30% (7%)	20% (6%)
CSC	225	25% (9%)	31% (7%)	31% (10%)	18% (8%)
CEC	40	27% (10%)	30% (8%)	34% (8%)	21% (8%)
CWC	45	29% (7%)	35% (8%)	30% (8%)	23% (13%)

[a]Values are given as mean ratios (standard deviations). N is the number of available hourly data points.
[b]Upslope equals 0800–1959 local time (Beijing time); downslope equals 2000–0759 local time.

3.3.2. NO_y Speciation

[35] In this section, we investigate the partitioning of NO_y at WLG, and compare the results with measurements taken at other remote high-altitude sites in the Northern Hemisphere. Table 5 summarizes the proportions of individual NO_y species at WLG for the whole data set and for the five air mass groups. Table 4 compares the NO_y partitioning data from WLG with those obtained from other remote areas of the Northern Hemisphere. At WLG, PAN and NO_3^- were the most abundant reactive nitrogen compounds, with average proportions (±standard deviation) of 32% (±8%) and 31% (±9%), followed by NO_x (24% ± 10%) and HNO_3 (20% ± 9%). The sum of NO_x, PAN, HNO_3, and NO_3^- accounted for the whole of the measured total NO_y. Our previous measurements using sampling canisters in 2003 indicated that the mixing ratios of seven C_1-C_5 alkyl nitrates at WLG were very low (mean = 10.8 pptv) accounting for < 1% of the measured NO_y.

[36] It is evident from Table 5 that although reactive nitrogen is principally emitted as NO, it largely exists in its secondary reservoir forms at WLG. This is consistent with the fact that air parcels are well processed photochemically during long range transport to the WLG site. The low NO_x/NO_y ratios (24% ± 10%) at WLG are comparable to those measured at other remote continental sites, such as ~22% at Jungfraujoch [*Zellweger et al.*, 2000] and ~30% at Mount Cimone [*Fischer et al.*, 2003], whereas much lower values (6–14%) have been observed in the more remote marine free troposphere (e.g., Mauna Loa, Pico Mountain, and TRACE P aircraft; see Table 4). Of the various air masses sampled at WLG, the CA air mass coming from the sparsely inhabited western regions had a lower ratio of NO_x/NO_y (12% ± 6%) than the other four air mass categories (24–29%).

[37] Among the secondary NO_y species, inorganic nitrate (HNO_3 20% plus NO_3^- 31%) was more abundant at WLG. This result is in good agreement with other measurements taken at remote, midlatitude sites such as Mauna Loa, Pico Mountain, and on the TRACE-P and INTEX-A aircraft, where inorganic nitrate made up 48–74% of NO_y (see Table 4). In contrast, higher PAN/NO_y ratios (55–77%) have been widely observed at high altitudes and latitudes in the Northern Hemisphere (e.g., Summit, Greenland; Goose Bay, Labrador). The temperature dependent decomposition of PAN is believed to be an important factor governing this latitudinal distribution of NO_y partitioning.

[38] An interesting result regarding the NO_y budget at WLG is that inorganic nitrate largely existed in the particle phase, with an average particulate to total nitrate ratio, i.e., $NO_3^-/(NO_3^- + HNO_3)$, of 0.62 (±0.13). It is distinctly different from the observations made at other remote sites (e.g., Mauna Loa, Pico Mountain, and the TRACE P and INTEX A missions; see Table 4), which found that the majority of inorganic nitrate was present in the gaseous phase. Instead, the pattern at WLG is quite similar to those usually observed at urban and pollution affected locations, where high levels of gaseous NH_3 and/or mineral particles are present [*Song and Carmichael*, 2001]. Previous measurements using filter based methods have also demonstrated the dominance of aerosol NO_3^- in the nitrate partitioning at WLG [*Xue*, 2002; *Ma et al.*, 2003]. *Ma et al.* [2003] reported a typical particulate to total nitrate ratio of ~0.9 for an autumn-winter campaign, with NO_3^- being present in both fine particles and coarse modes. They suggested that nitrate in fine particles may be produced by the reaction of gaseous HNO_3 with NH_3, whereas coarse nitrate may be generated by the condensation of HNO_3 on the surface of mineral particles. Livestock husbandry and agriculture are the main activities on the Plateau, both of which are major emission sources of NH_3. As indicated in section 3.3.1, the concentrations of NH_3 are indeed very high at WLG. Furthermore, particles at WLG have been shown to be predominantly from natural sources, such as soil and crust [*Gao and Anderson*, 2001]. The large abundances of NH_3 and crustal aerosols provide sufficient neutralizers for gaseous HNO_3, thus favoring the formation of particulate nitrate and explaining its greater presence in NO_y at WLG.

4. Summary and Conclusions

[39] In summer 2006, speciated reactive nitrogen compounds (NO, NO_2, PAN, HNO_3, and NO_3^-) were continuously measured in conjunction with total reactive nitrogen (NO_y), ozone, and carbon monoxide at WLG on the Qinghai-Tibetan Plateau. The data were analyzed to help further understand the origins of surface ozone and reactive nitrogen, and to investigate nitrogen partitioning in the remote free troposphere of western China.

[40] The mean concentrations of O_3, CO, and daytime NO were 59 ppbv, 149 ppbv, and 71 pptv, respectively, which were significantly higher than those measured during the previous study in summer 2003. More frequent anthropogenic impact from central and eastern China was observed at WLG in summer of 2006 (~55%) than that of 2003 (~25%). Varied diurnal patterns were observed for the different NO_y constituents. Ozone production efficiencies of 7.7–11.3 were calculated for the air masses recently influenced by the anthropogenic emissions in central and eastern China.

[41] Despite the more frequent transport of anthropogenic pollution, the NO_y levels in the 2006 study (mean = 1.44 ppbv) were substantially lower than those observed in 2003 (mean = 3.60 ppbv). Changes in emissions from soil and anthropogenic sources are unlikely to account for the large discrepancy between the two study periods. Based on the recent test results on NH_3 interference in MoO converters, we suspect that the abnormally high NO_y values in 2003 were due to NH_3 interference in the particular converter used.

[42] NO_y partitioning was investigated for the first time in the remote free troposphere in western China. PAN and particulate NO_3^- were the dominant NO_y species in summer at WLG, and comprised on average 32% and 31% of the measured NO_y, followed by NO_x (24%) and HNO_3 (20%). Compared with results obtained from other remote, high-altitude sites in the Northern Hemisphere, particulate nitrate made a greater contribution to NO_y, which can be attributed to the high abundance of NH_3 and mineral particles over the Plateau.

[43] Further analysis of backward trajectories for the recent 10 years indicated that WLG was frequently (~50% of air masses) influenced by the air from the east, suggesting an important role of anthropogenic emissions in central and eastern China in shaping the summertime surface ozone and other atmospheric trace constituents at WLG and over the Tibetan Plateau.

[44] **Acknowledgments.** We are grateful to the staff at the WLG Observatory for their help throughout the field campaign, to Hongchao Zuo for assistance with securing shipment and customs clearance for the instruments, and to NOAA Air Resources Laboratory (ARL) for providing the HYSPLIT model. The work was funded by the National Basic Research Program (973 Program) of China (2005CB422203) and the Hong Kong Polytechnic University (1-BB94).

References

Anlauf, K., H. A. Wiebe, and P. Fellin (1986), Characterization of several integrative sampling methods for nitric acid, sulphur dioxide and atmospheric particles, *J. Air Pollut. Control Assoc.*, *36*, 715–723.

Appel, B., Y. Tokiwa, and M. Haik (1981), Sampling of nitrates in ambient air, *Atmos. Environ.*, *15*, 283–289, doi:10.1016/0004-6981(81)90029-9.

Atlas, E., and B. A. Ridley (1996), The Mauna Loa Observatory Photochemistry Experiment: Introduction, *J. Geophys. Res.*, *101*(D9), 14,531–14,541, doi:10.1029/96JD01203.

Chin, M., D. J. Jacob, J. W. Munger, D. D. Parrish, and B. G. Doddridge (1994), Relationship of ozone and carbon monoxide over North America, *J. Geophys. Res.*, *99*(D7), 14,565–14,573, doi:10.1029/94JD00907.

Crutzen, P. (1973), A discussion of the chemistry of some minor constituents in the stratosphere and troposphere, *Pure Appl. Geophys.*, *106*, 1385–1399, doi:10.1007/BF00881092.

Ding, A., and T. Wang (2006), Influence of stratosphere to troposphere exchange on the seasonal cycle of surface ozone at Mount Waliguan in western China, *Geophys. Res. Lett.*, *33*, L03803, doi:10.1029/2005GL024760.

Duderstadt, K., et al. (1998), Photochemical production and loss rates of ozone at Sable Island, Nova Scotia during the North Atlantic Regional Experiment (NARE) 1993 summer intensive, *J. Geophys. Res.*, *103*(D11), 13,531–13,555, doi:10.1029/98JD00397.

Fischer, H., et al. (2003), Ozone production and trace gas correlations during the June 2000 MINATROC intensive measurement campaign at Mt. Cimone, *Atmos. Chem. Phys.*, *3*, 725–738, doi:10.5194/acp-3-725-2003.

Fitz, D., K. Bumiller, and A. Lashgari (2003), Measurement of NO_y during the SCOS97 NARSTO, *Atmos. Environ.*, *37*, Suppl. 2, 119–134, doi:10.1016/S1352-2310(03)00385-6.

Ford, K. M., B. M. Campbell, P. B. Shepson, S. B. Bertman, R. E. Honrath, M. Peterson, and J. E. Dibb (2002), Studies of peroxyacetyl nitrate (PAN) and its interaction with the snowpack at Summit, Greenland, *J. Geophys. Res.*, *107*(D10), 4102, doi:10.1029/2001JD000547.

Gao, Y., and J. R. Anderson (2001), Characteristics of Chinese aerosols determined by individual particle analysis, *J. Geophys. Res.*, *106*(D16), 18,037–18,045, doi:10.1029/2000JD900725.

Goldan, P., W. C. Kuster, D. L. Albritton, F. C. Fehsenfeld, P. S. Connell, R. B. Norton, and B. J. Huebert (1983), Calibration and tests of the filter collection method for measuring clean air, ambient levels of nitric acid, *Atmos. Environ.*, *17*, 1355–1364, doi:10.1016/0004-6981(83)90410-9.

Hirsch, R. M., and E. J. Gilroy (1984), Methods of fitting a straight line to data: Examples in water resources, *Water Resour. Bull.*, *20*(5), 705–711.

Intergovernmental Panel on Climate Change (2007), *Climate Change 2007: The Physical Science Basis. Contribution of Working Group I to the Fourth Assessment Report of the Intergovernmental Panel on Climate Change*, Cambridge Univ. Press, Cambridge, U. K.

Jaeglé, L., D. J. Jacob, Y. Wang, A. J. Weinheimer, B. A. Ridley, T. L. Campos, G. W. Sachse, and D. E. Hagen (1998), Sources and chemistry of NO_x in the upper troposphere over the United States, *Geophys. Res. Lett.*, *25*(10), 1705–1708, doi:10.1029/97GL03591.

Kivekäs, N., J. Sun, M. Zhan, V. M. Kerminen, A. Hyvärinen, M. Komppula, Y. Viisanen, N. Hong, Y. Zhang, M. Kulmala, X. C. Zhang, Deli Geer, and H. Lihavainen (2009), Long term particle size distribution measurements at Mount Waliguan, a high altitude site in inland China, *Atmos. Chem. Phys.*, *9*, 5461–5474, doi:10.5194/acp-9-5461-2009.

Li, J., Z. Wang, H. Akimoto, J. Tang, and I. Uno (2009), Modeling of the impacts of China's anthropogenic pollutants on the surface ozone summer maximum on the northern Tibetan Plateau, *Geophys. Res. Lett.*, *36*, L24802, doi:10.1029/2009GL041123.

Li, S., J. Tang, H. Xue, and D. Toom Sauntry (2000), Size distribution and estimated optical properties of carbonate, water soluble organic carbon, and sulfate in aerosols at a remote high altitude site in western China, *Geophys. Res. Lett.*, *27*(8), 1107–1110, doi:10.1029/1999GL010929.

Ma, J., J. Tang, S. M. Li, and M. Z. Jacobson (2003), Size distributions of ionic aerosols measured at Waliguan Observatory: Implication for nitrate gas to particle transfer processes in the free troposphere, *J. Geophys. Res.*, *108*(D17), 4541, doi:10.1029/2002JD003356.

Ma, J., X. Zheng, and X. Xu (2005), Comment on "Why does surface ozone peak in summertime at Waliguan?" by Bin Zhu et al., *Geophys. Res. Lett.*, *32*, L01805, doi:10.1029/2004GL021683.

Meng, Z., X. B. Xu, T. Wang, X. Y. Zhang, X. L. Yu, S. F. Wang, W. L. Lin, Y. Z. Chen, Y. A. Jiang, and X. Q. An (2010), Ambient sulfur dioxide, nitrogen dioxide, and ammonia at ten background and rural sites in China during 2007–2008, *Atmos. Environ.*, *44*, 2625–2631, doi:10.1016/j.atmosenv.2010.04.008.

Monks, P. S. (2000), A review of the observations and origins of the spring ozone maximum, *Atmos. Environ.*, *34*, 3545–3561, doi:10.1016/S1352 2310(00)00129 1.

Mu, Y., X. Pang, J. Quan, and X. Zhang (2007), Atmospheric carbonyl compounds in Chinese background area: A remote mountain of the Qinghai Tibetan Plateau, *J. Geophys. Res.*, *112*, D22302, doi:10.1029/2006JD008211.

Munger, J. W., D. J. Jacob, S. M. Fan, A. S. Colman, and J. E. Dibb (1999), Concentrations and snow atmosphere fluxes of reactive nitrogen at Summit, Greenland, *J. Geophys. Res.*, *104*(D11), 13,721–13,734, doi:10.1029/1999JD900192.

National Research Council (1991), *Rethinking the Ozone Problem in Urban and Regional Air Pollution*, Natl. Acad. Press, Washington, D. C.

Neuman, J. A., et al. (2006), Reactive nitrogen transport and photochemistry in urban plumes over the North Atlantic Ocean, *J. Geophys. Res.*, *111*, D23S54, doi:10.1029/2005JD007010.

Ogi, M., J. Yamazaki, and Y. Tachibana (2005), The summer northern annular mode and abnormal summer weather in 2003, *Geophys. Res. Lett.*, *32*, L04706, doi:10.1029/2004GL021528.

Qinghai Bureau of Statistics (2007), *Qinghai Statistical Yearbook 2007* (in Chinese), China Stat. Press, Beijing.

Saigusa, N., et al. (2010), Impact of meteorological anomalies in the 2003 summer on gross primary productivity in East Asia, *Biogeosciences*, *7*, 641–655, doi:10.5194/bg-7-641-2010.

Singh, H. B., and L. J. Salas (1983), Peroxyacetyl nitrate in the free troposphere, *Nature*, *302*, 326–328, doi:10.1038/302326a0.

Singh, H. B., L. J. Salas, and W. Viezee (1986), Global distribution of peroxyacetyl nitrate, *Nature*, *321*, 588–591, doi:10.1038/321588a0.

Singh, H., et al. (1994), Summertime distribution of PAN and other reactive nitrogen species in the northern high latitude atmosphere of eastern Canada, *J. Geophys. Res.*, *99*(D1), 1821–1835, doi:10.1029/93JD00946.

Singh, H. B., et al. (1996), Reactive nitrogen and ozone over the western Pacific: Distribution, partitioning, and sources, *J. Geophys. Res.*, *101*(D1), 1793–1808, doi:10.1029/95JD01029.

Singh, H. B., et al. (2007), Reactive nitrogen distribution and partitioning in the North American troposphere and lowermost stratosphere, *J. Geophys. Res.*, *112*, D12S04, doi:10.1029/2006JD007664.

Song, C., and G. R. Carmichael (2001), A three dimensional modeling investigation of the evolution processes of dust and sea salt particles in East Asia, *J. Geophys. Res.*, *106*(D16), 18,131–18,154, doi:10.1029/2000JD900352.

Stohl, A., et al. (2003), Stratosphere troposphere exchange: A review, and what we have learned from STACCATO, *J. Geophys. Res.*, *108*(D12), 8516, doi:10.1029/2002JD002490.

Streets, D. G., et al. (2003), An inventory of gaseous and primary aerosol emissions in Asia in the year 2000, *J. Geophys. Res.*, *108*(D21), 8809, doi:10.1029/2002JD003093.

Talbot, R., et al. (2003), Reactive nitrogen in Asian continental outflow over the western Pacific: Results from the NASA Transport and Chemical

Evolution over the Pacific (TRACE P) airborne mission, *J. Geophys. Res.*, *108*(D20), 8803, doi:10.1029/2002JD003129.

Tang, J., Y. P. Wen, X. B. Xu, X. D. Zheng, S. Guo, and Y. C. Zhao (1995), China Global Atmosphere Watch Baseline Observatory and its measurement program, in *CAMS Annual Report 1994–95*, pp. 56–65, China Meteorol. Press, Beijing.

Trainer, M., et al. (1993), Correlation of ozone with NO_y in photochemically aged air, *J. Geophys. Res.*, *98*(D2), 2917–2925, doi:10.1029/92JD01910.

Val Martin, M., R. E. Honrath, R. C. Owen, and Q. B. Li (2008), Seasonal variation of nitrogen oxides in the central North Atlantic lower free troposphere, *J. Geophys. Res.*, *113*, D17307, doi:10.1029/2007JD009688.

Wang, T., V. T. F. Cheung, K. S. Lam, G. L. Kok, and J. M. Harris (2001), The characteristics of ozone and related compounds in the boundary layer of the South China coast: Temporal and vertical variations during autumn season, *Atmos. Environ.*, *35*, 2735–2746, doi:10.1016/S1352-2310(00)00411-8.

Wang, T., H. L. A. Wong, J. Tang, A. Ding, W. S. Wu, and X. C. Zhang (2006), On the origin of surface ozone and reactive nitrogen observed at a remote mountain site in the northeastern Qinghai Tibetan Plateau, western China, *J. Geophys. Res.*, *111*, D08303, doi:10.1029/2005JD006527.

Wang, T., et al. (2010), Air quality during the 2008 Beijing Olympics: Secondary pollutants and regional impact, *Atmos. Chem. Phys.*, *10*, 7603–7615, doi:10.5194/acp-10-7603-2010.

Wang, Y., J. A. Logan, and D. J. Jacob (1998), Global simulation of tropospheric O_3 NO_x hydrocarbon chemistry: 2. Model evaluation and global ozone budget, *J. Geophys. Res.*, *103*(D9), 10,727–10,755, doi:10.1029/98JD00157.

Williams, E. J., D. D. Parrish, M. P. Buhr, F. C. Fehsenfeld, and R. Fall (1988), Measurement of soil NO_x emissions in central Pennsylvania, *J. Geophys. Res.*, *93*(D8), 9539–9546, doi:10.1029/JD093iD08p09539.

Williams, E. J., J. M. Roberts, K. Baumann, S. B. Bertman, S. Buhr, R. B. Norton, and F. C. Fehsenfeld (1997), Variations in NO_y composition at Idaho Hill, Colorado, *J. Geophys. Res.*, *102*(D5), 6297–6314, doi:10.1029/96JD03252.

Williams, E. J., et al. (1998), Intercomparison of ground based NO_y measurement techniques, *J. Geophys. Res.*, *103*(D17), 22,261–22,280, doi:10.1029/98JD00074.

Wood, E. C., et al. (2009), A case study of ozone production, nitrogen oxides, and the radical budget in Mexico City, *Atmos. Chem. Phys.*, *9*, 2499–2516, doi:10.5194/acp-9-2499-2009.

Xue, H. S. (2002), Observational study of chemical characteristics of aerosol and trace gases of HNO_3, SO_2, at Mt. Waliguan (in Chinese), Master's thesis, Beijing Univ., Beijing.

Yienger, J., and H. Levy II (1995), Empirical model of global soil biogenic NO_x emissions, *J. Geophys. Res.*, *100*(D6), 11,447–11,464, doi:10.1029/95JD00370.

Zanis, P., A. Ganser, C. Zellweger, S. Henne, M. Steinbacher, and J. Staehelin (2007), Seasonal variability of measured ozone production efficiencies in the lower free troposphere of central Europe, *Atmos. Chem. Phys.*, *7*, 223–236, doi:10.5194/acp-7-223-2007.

Zellweger, C., M. Ammann, B. Buchmann, P. Hofer, M. Lugauer, R. Rüttimann, N. Streit, E. Weingartner, and U. Baltensperger (2000), Summertime NO_y speciation at the Jungfraujoch, 3580 m above sea level, Switzerland, *J. Geophys. Res.*, *105*(D5), 6655–6667, doi:10.1029/1999JD901126.

Zellweger, C., J. Forrer, P. Hofer, S. Nyeki, B. Schwarzenbach, E. Weingartner, M. Ammann, and U. Baltensperger (2003), Partitioning of reactive nitrogen (NO_y) and dependence on meteorological conditions in the lower free troposphere, *Atmos. Chem. Phys.*, *3*, 779–796, doi:10.5194/acp-3-779-2003.

Zhang, J., et al. (2009), Continuous measurement of peroxyacetyl nitrate (PAN) in suburban and remote areas of western China, *Atmos. Environ.*, *43*, 228–237, doi:10.1016/j.atmosenv.2008.09.070.

Zhang, Q., et al. (2007), NO_x emission trends for China, 1995–2004: The view from the ground and the view from space, *J. Geophys. Res.*, *112*, D22306, doi:10.1029/2007JD008684.

Zhang, Q., et al. (2009), Asian emissions in 2006 for the NASA INTEX B mission, *Atmos. Chem. Phys.*, *9*, 5131–5153, doi:10.5194/acp-9-5131-2009.

Zhou, L., D. E. J. Worthy, P. M. Lang, M. K. Ernst, X. C. Zhang, Y. P. Wen, and J. L. Li (2004), Ten years of atmospheric methane observations at a high elevation site in western China, *Atmos. Environ.*, *38*, 7041–7054, doi:10.1016/j.atmosenv.2004.02.072.

Zhu, B., H. Akimoto, Z. Wang, K. Sudo, J. Tang, and I. Uno (2004), Why does surface ozone peak in summertime at Waliguan?, *Geophys. Res. Lett.*, *31*, L17104, doi:10.1029/2004GL020609.

Deliger, China GAW Baseline Observatory, Qinghai Meteorological Bureau, Xining, Qinghai 810001, China.

A. J. Ding, Institute for Climate and Global Change Research, Nanjing University, Nanjing, Jiangsu 210093, China.

C. N. Poon, T. Wang, W. S. Wu, and J. M. Zhang, Department of Civil and Structural Engineering, Hong Kong Polytechnic University, Hung Hom, Kowloon, Hong Kong, China. (cetwang@polyu.edu.hk)

J. Tang and X. C. Zhang, Centre for Atmosphere Watch and Services, Key Laboratory for Atmospheric Chemistry, Chinese Academy of Meteorological Sciences, Beijing 100081, China.

W. X. Wang, L. K. Xue, Q. Z. Zhang, and X. H. Zhou, Environment Research Institute, Shandong University, Ji'nan, Shandong 250100, China.